Title

Surface Cytotoxic T Lymphocyte–associated Antigen 4 Partitions Within Lipid Rafts and Relocates to the Immunological Synapse under Conditions of Inhibition of T Cell Activation

Journal

Journal of Experimental Medicine, 195(10)

ISSN

0022-1007

Authors

Darlington, Peter J
Baroja, Miren L
Chau, Thu A
et al.

Publication Date

2002-05-20

DOI

10.1084/jem.20011868

Peer reviewed

Surface Cytotoxic T Lymphocyte–associated Antigen 4 Partitions Within Lipid Rafts and Relocates to the Immunological Synapse under Conditions of Inhibition of T Cell Activation

Peter J. Darlington,[1] Miren L. Baroja,[1] Thu A. Chau,[1] Eric Siu,[1] Vincent Ling,[2] Beatriz M. Carreno,[2] and Joaquín Madrenas[1]

[1] *The Biotherapeutics and Transplantation and Immunobiology Groups, The John P. Robarts Research Institute, and The Departments of Microbiology and Immunology, and Medicine, The University of Western Ontario, London, Ontario N6A 5K8, Canada*

[2] *Wyeth-Genetics Institute Incorporated, Cambridge, MA 02140*

Abstract

T cell activation through the T cell receptor (TCR) involves partitioning of receptors into discrete membrane compartments known as lipid rafts, and the formation of an immunological synapse (IS) between the T cell and antigen-presenting cell (APC). Compartmentalization of negative regulators of T cell activation such as cytotoxic T lymphocyte–associated antigen-4 (CTLA-4) is unknown. Recent crystal structures of B7-ligated CTLA-4 suggest that it may form lattices within the IS which could explain the mechanism of action of this molecule. Here, we show that after T cell stimulation, CTLA-4 coclusters with the TCR and the lipid raft ganglioside GM1 within the IS. Using subcellular fractionation, we show that most lipid raft-associated CTLA-4 is on the T cell surface. Such compartmentalization is dependent on the cytoplasmic tail of CTLA-4 and can be forced with a glycosylphosphatidylinositol-anchor in CTLA-4. The level of CTLA-4 within lipid rafts increases under conditions of APC-dependent TCR–CTLA-4 coligation and T cell inactivation. However, raft localization, although necessary for inhibition of T cell activation, is not sufficient for CTLA-4–mediated negative signaling. These data demonstrate that CTLA-4 within lipid rafts migrates to the IS where it can potentially form lattice structures and inhibit T cell activation.

Key words: CTLA-4 • T cells • lipid rafts • immunological synapse • T cell inactivation

Introduction

An increasing body of evidence indicates that T cell activation involves lateral migration of many molecules associated with TCR-mediated signaling. When T cells are stimulated with planar lipid bilayers or APCs possessing antigenic peptide–MHC, a highly ordered macromolecular interface termed immunological synapse (IS)* forms between the T cell and the APC surface (1). The IS is composed of a central core containing TCR/CD3, PKCθ, lck, fyn, and CD28, surrounded by a ring enriched for LFA-1 talin, and CD43 (2–5). The organization of such an interface is determined in part by the intermembrane dimensions of the synapse, which may exclude complexes that encompass more than 15 nm (6). At a submicroscopic level, formation of an IS correlates with clustering of glycolipid-enriched microdomains known as lipid rafts. These domains move into the IS in response to CD3 and CD28 ligation (7). Lipid rafts are enriched with signaling molecules critical for TCR-mediated signaling such as lck, linker for activation of T cells (LAT), and PKCθ (8–10), and their biological integrity is essential for proper TCR-mediated signaling (8, 11).

In the context of the lipid raft/IS paradigm, the compartmentalization of negative regulators of T cell activation remains largely unexplored. Establishing this compartmentalization may provide insights into their mechanism

P.J. Darlington and M.L. Baroja contributed equally to this work.

Address correspondence to J. Madrenas, Robarts Research Institute, RRI-2.05, P.O. Box 5015, 100 Perth Dr., London, ON N6A 5K8, Canada. Phone: 519-663-5777, ext. 34242; Fax: 519-663-3789; E-mail: madrenas@rri.ca

**Abbreviations used in this paper:* ANOVA, analysis of variance; CTLA-4, CTL-associated antigen 4; GPI, glycosylphosphatidylinositol; IS, immunological synapse; LAT, linker for activated T cells; SEE, Staphylococcal enterotoxin E.

 J. Exp. Med. © The Rockefeller University Press • 0022-1007/2002/05/1337/11 $5.00
Volume 195, Number 10, May 20, 2002 1337–1347
http://www.jem.org/cgi/doi/10.1084/jem.20011868

of action as well as help us to understand the structural nature of receptor-mediated T cell activation. To address this issue, we looked at one of the main negative regulators of T cell activation, CTL-associated antigen 4 (CTLA-4). CTLA-4 is an activation-induced, type 1 transmembrane protein expressed by T cells (12). Upon coligation with the TCR, CTLA-4 blocks IL-2 gene transcription and prevents the entry of T cells into the growth phase beyond G1/G0 leading to inhibition of T cell proliferation (13, 14). Such an inhibitory effect on T cell activation is illustrated by the unregulated lymphoproliferation and multiorgan autoimmunity observed in CTLA-4–deficient mice (15–18).

CTLA-4 can inhibit T cell responses by two different mechanisms (for a review, see reference 19). One mechanism involves antagonism of B7-CD28–mediated costimulatory signals by CTLA-4 (20), which occurs because CTLA-4 has a much higher affinity for B7 than does CD28 (21, 22). This mechanism is only dependent on the extracellular domain of CTLA-4 and is operational in a manner directly proportional to the level of surface expression (20). A second mechanism by which CTLA-4 can inactivate T cells involves the delivery of a negative signal (23–26). In contrast to CTLA-4–mediated sequestration of B7, negative signaling by CTLA-4 requires the cytoplasmic tail of CTLA-4 and is operational at low levels of surface expression (20). However, the precise molecular nature of CTLA-4–mediated negative signaling remains controversial (23, 24, 26–28).

Recently, several crystal structures of CTLA-4 and the CTLA-4–B7 complex have been reported (29–32). These structures indicate that the predicted intermembrane distance of the B7–CTLA-4 complex may be in the range of the MHC–TCR interaction (~130–150 Å) and would thus fit within the central core of the IS. More importantly, the topology of CTLA-4 dimers ligated with B7 dimers suggest that CTLA-4 may form high order oligomers at the IS. If such a lattice forms, it may lead to disruption of the structure and/or function of the synapse. To test this hypothesis, we examined the distribution of CTLA-4 on the T cell surface under conditions of CTLA-4–mediated inhibition of T cell activation. We report that CTLA-4 colocalizes with TCR/CD3 complex and the ganglioside GM1 within the IS upon exposure to superantigen and APC. When lipid rafts were analyzed in conditions of CTLA-4–mediated inhibition, we found that although most CTLA-4 partitioned in detergent soluble fractions, a detectable fraction of the surface pool of CTLA-4 was within lipid rafts. Moreover, CTLA-4 in lipid rafts was homodimeric and its levels increased upon exposure to superantigen and APCs. The partition of CTLA-4 within lipid rafts was dependent on the cytoplasmic tail of CTLA-4. The presence of CTLA-4 in lipid rafts was necessary, but not sufficient for T cell inhibition to occur since a glycosylphosphatidylinositol (GPI)-anchored version of CTLA-4 was targeted exclusively to lipid rafts but failed to deliver an inhibitory signal.

Materials and Methods

Cell Lines and Transfectants. The human leukemia T cell line Jurkat, E6.1 was obtained from the American Type Culture Collection, and maintained in RPMI with 10% FCS. Jurkat T cells expressing doxycycline-inducible wild-type or tailless CTLA-4 molecules (that have the transmembrane but not the cytoplasmic region of CTLA-4) have been described previously (24). New for the studies reported here is the human GPI-anchored CTLA-4, which is a fusion construct comprised of sequences corresponding to a Kozak sequence and the extracellular region of human CTLA4 (GenBank/EMBL/DDBJ accession no. AF414120) fused by a spacer sequence to the sequence corresponding to the carboxy-terminus of the glycosylphosphatidylinositol-linked isoform of CD58/LFA-3 (GenBank/EMBL/DDBJ accession no. XM_040693, positions 548–792). Human CTLA-4-gpi was subcloned into the doxycycline inducible vector pBIG2i at the XhoI multiple cloning site. Transfection and subcloning was done as described previously (24). CTLA-4 was induced by overnight incubation with doxycycline (Sigma-Aldrich) at a concentration of 100 ng/ml for IL-2 production assays, or 5 μg/ml for biochemical experiments. The B lymphoblastoid cell line LG2, which expresses high levels of HLA-DR1 and B7, was provided by Dr. Eric Long (Molecular and Cellular Immunology Section, Laboratory of Immunogenetics, National Institute of Allergy and Infectious Diseases, National Institutes of Health, Rockville, MD) and maintained in RPMI with 10% FCS.

Antibodies and Reagents. The following antibodies were used in this study: T cell functional assays were performed using beads coated with monoclonal antibodies against human CD3ε (UCHT-1; BD PharMingen), human CTLA-4 (anti-CTLA-4–20A; Wyeth-Genetics Institute Inc.), or against HLA-class I molecules (G46–2.6; BD PharMingen). A monoclonal antibody against human CD28 (CD28.2), FITC-labeled anti-CD3 (UCHT-1), and PE-labeled anti-CTLA-4 (BNI3) antibodies were purchased from BD PharMingen. A mouse anti–human ScFv CTLA-4 F′ab fragment was generated by recombinant technology and provided by Genetics Institute. A FITC-labeled antibody against pan-CD45 (HI30) and a FITC-labeled antibody against CD43 (1G10) were purchased from BD PharMingen. GM1 analysis was performed with FITC-cholera toxin B subunit (Molecular Probes). CTLA-4 was immunoprecipitated with the anti–human CTLA-4–24 monoclonal antibody, and immunoblotted with the anti-CTLA-4–11 monoclonal antibody, both from Wyeth-Genetics Institute Inc. Appropriate isotype-matched antibody controls were purchased from Southern Biotechnology Associates, Inc. ERK-1/-2 were blotted using a rabbit antiserum from StressGen Biotechnologies. Biotinylated molecules were immunoprecipitated with an antibody against biotin from Jackson Immunoresearch Laboratories.

Inhibition of IL-2 Production by CTLA-4. To assay inhibition of superantigen-mediated stimulation by CTLA-4, 0.5×10^6 transfectants were incubated for 48 h with 0.25×10^6 LG2 plus 5 ng/ml staphylococcal enterotoxin E (SEE; Toxin Technology Inc.), with or without 100 ng/ml doxycycline. To assay for inhibition of IL-2 production by CTLA-4–mediated negative signaling, Jurkat T cells (5×10^5/group) were incubated with anti-CD3 and anti-HLA-class I–coated beads or with anti-CD3 and anti-CTLA-4–coated beads, in 24-well plates for 48 h in the presence of soluble anti-CD28 monoclonal antibodies (20 μg/ml), as described previously (20, 33). IL-2 in the supernatants was analyzed by ELISA. For the blocking of CTLA-4–mediated inhibition of IL-2 production, 0.5×10^6 Jurkat T cells were preincubated with 100 ng/ml of doxycycline and a total of 10 μg of anti-

CTLA-4 ScFv CTLA-4 F′ab fragment. After 30 min of preincubation, antibody-coated beads plus soluble anti-CD28 antibody or APCs and SEE were added to the samples.

Confocal Microscopy. 35-mm glass bottom microwell dishes, (MatTek Corp.) were coated overnight with poly-L-lysine (Sigma-Aldrich). T cells (1.0×10^6) were incubated on the plates for 30 min before adding LG2 cells that had been preincubated with 100 ng/ml SEE for 30 min. Dishes were washed twice with PBS plus 1% FCS, stained with PE-labeled anti-CTLA-4 (30 min on ice) followed by FITC-labeled anti-CD3 or FITC-labeled cholera toxin B subunits. Image capture was done with a confocal microscope (Carl Zeiss, Inc.) and analyzed with the LSM 510 software (Carl Zeiss, Inc.; Microsoft). Quantitation of CD3-CTLA-4 colocalization at the putative immunological synapse was performed on at least 100 T cell–APC doublets. Capping for each molecule at the interface between the T cell and the APC was scored when the staining was visible on <50% of the T cell surface.

Flow Cytometry. Jurkat T cells (1.0×10^6/group) were washed twice with PBS and stained with FITC-labeled anti-CD3, FITC-labeled anti-CD28, PE-labeled anti–CTLA-4, or FITC-labeled anti-CD45 in ice for 30 min. Samples were then washed twice in PBS and analyzed by flow cytometry (FACScan™ and CELLQuest™ software; BD PharMingen).

Lipid Raft Isolation and Biochemistry. LG2 cells (0.5×10^6/ml) in 6-well plates were preincubated with 100 ng/ml of SEE for 30 min. Next, Jurkat T cells (40×10^6 per group) were added at the ratio of 5:1 and incubated for 30 min. Cells were pelleted, washed once in cold PBS, and used for lipid raft isolation. Lipid raft isolation was done as reported previously (8). Briefly, 40–80 $\times$ 10^6 T cells were lysed in buffer containing 0.5% Triton X-100, 25 mM MES, 150 mM NaCl, 1 mM Na_3VO_4, 2 mM EDTA, 1 mM PMSF, and 1 μg/ml aprotinin. Lysates were then homogenized, mixed with equal volume of 85% wt/vol sucrose, and put under a step gradient consisting of 35% wt/vol and 5% wt/vol layers of sucrose in MBS (25 mM MES, 150 ml NaCl, pH 6.5) supplemented with 1 mM Na_3VO_4 and 2 mM EDTA. Samples were then ultracentrifuged for 16–18 h at 200,000 *g*, 4°C. 12 1-ml fractions were taken starting at the top, with fraction 5 containing the cloudy band indicative of rafts and fraction 12 taken as the soluble fraction. Fraction aliquots were mixed with 4× sample buffer (8% SDS, 8% 2-mercaptoethanol, 250 mM tris, 40% glycerol, 2% bromophenol blue, dd-H_2O) to a final dilution of 1×. Immunoprecipitation was done as described previously (34) except that lipid raft fractions were first pelleted by adding equal volume of MBS, centrifuging for 10 min at 14,000 rpm, 4°C on a table top microcentrifuge, and resuspended in 1 ml lysis buffer. Fractions were run on SDS-PAGE and immunoblotted as described previously (34). Where indicated, samples were diluted by 10 with 1× sample buffer. Chemiluminescence signals were scanned with a GS-700 Imaging densitometer and analyzed by Multi Analyst software (Bio-Rad Laboratories). Mean OD was measured for each band and corrected for dilution where applicable. The percentage of total CTLA-4 within lipid rafts was determined using the conversion formula (mean OD rafts)/(mean OD soluble + mean OD raft) $\times$ 100%.

Cell Surface Biotinylation. To biotinylate molecules on the surface of Jurkat T cells, cells were washed twice with 1× PBS (1 ml) and rotated for 30 min in 0.5 mg/ml EZ-link Sulfo-NHS-LC-biotin (Pierce Chemical Co.) in PBS, pH 8.0, at a cell concentration of 25×10^6/ml. Samples were washed three times with 1× PBS before raft isolation. In experiments looking at the percentage of total CTLA-4 expressed on the cell surface, cell lysates from biotinylated cells were immunoprecipitated with antibodies against biotin or against CTLA-4, and these immunoprecipitates were subsequently blotted with CTLA-4. Additionally, CTLA-4 immunoprecipitates of raft and soluble fractions from biotinylated wild-type CTLA-4–transfected T cells in the presence or absence of doxycycline were prepared and immunoblotted with HRP-conjugated avidin (Bio-Rad Laboratories). CTLA-4 signals or avidin signals in each group were analyzed by densitometry using the Phoretix 1D advanced v5.1 software (Nonlinear USA Inc.). In experiments looking at the effect of T cell stimulation on CTLA-4 distribution, biotinylation was performed under the same conditions, immediately after SEE and APC stimulation using 200×10^6 doxycycline-induced, wild-type CTLA-4 transfected T cells, 60×10^6 tailless CTLA-4 transfected T cells, or GPI-anchored CTLA-4 T cell transfectants. All biotinylation steps were done at room temperature to prevent biotin precipitation.

Results

Wild-Type CTLA-4 Redistributes to the Immunological Synapse upon Coligation with the TCR. The main obstacle to assess the membrane distribution of CTLA-4 has been the low, transient level of CTLA-4 expression on the surface of primary T lymphocytes. Of the very low levels of CTLA-4 produced, only 5% reaches the membrane and is rapidly internalized (21). To circumvent this problem, we used Jurkat T cells which do not express endogenous CTLA-4, and stably transfected with a doxycycline-inducible expression vector for wild-type CTLA-4 or mutants of CTLA-4. This system provides a powerful model to address CTLA-4 structure-function analysis as described previously (20, 24). The three transfectants for the studies reported here include wild-type CTLA-4, CTLA-4 without the cytoplasmic tail (so called tailless CTLA-4), and a newly generated chimerical version of CTLA-4 consisting of its extracellular domain fused to the CD58 GPI-anchor.

The expression of CTLA-4, CD3, CD28, and CD45 in the absence or presence of doxycycline is shown in Fig. 1 A for representative stably transfected T cell clones. Without doxycycline, wild-type CTLA-4 transfected cells expressed barely detectable levels of the recombinant protein. In contrast, tailless CTLA-4 and GPI-anchored CTLA-4 Jurkat T cell transfectants had a detectable degree of "leakiness", which was amplified by the inability of these CTLA-4 molecules to be endocytosed (35, 36). Upon induction with doxycycline, a significant increase in surface expression of CTLA-4 was detected in all the transfectants (Fig. 1 A). As Jurkat T cells do not express endogenous CTLA-4, all of the CTLA-4 expression comes from the transfected cDNA. Doxycycline did not affect the surface levels of CD3 or CD28 (Fig. 1 A). As expected, the percentage of total CTLA-4 expressed on the cell surface varied for each one of the transfectants (20–25% for wild-type CTLA-4, close to 100% for the tailless CTLA, and around 80% for the GPI-anchored CTLA-4) even though the total levels of CTLA-4 in the three T cell transfectants after doxycycline induction were comparable (24; Fig. 1 B). Appropriate isotype-matched immunoprecipitation controls showed no

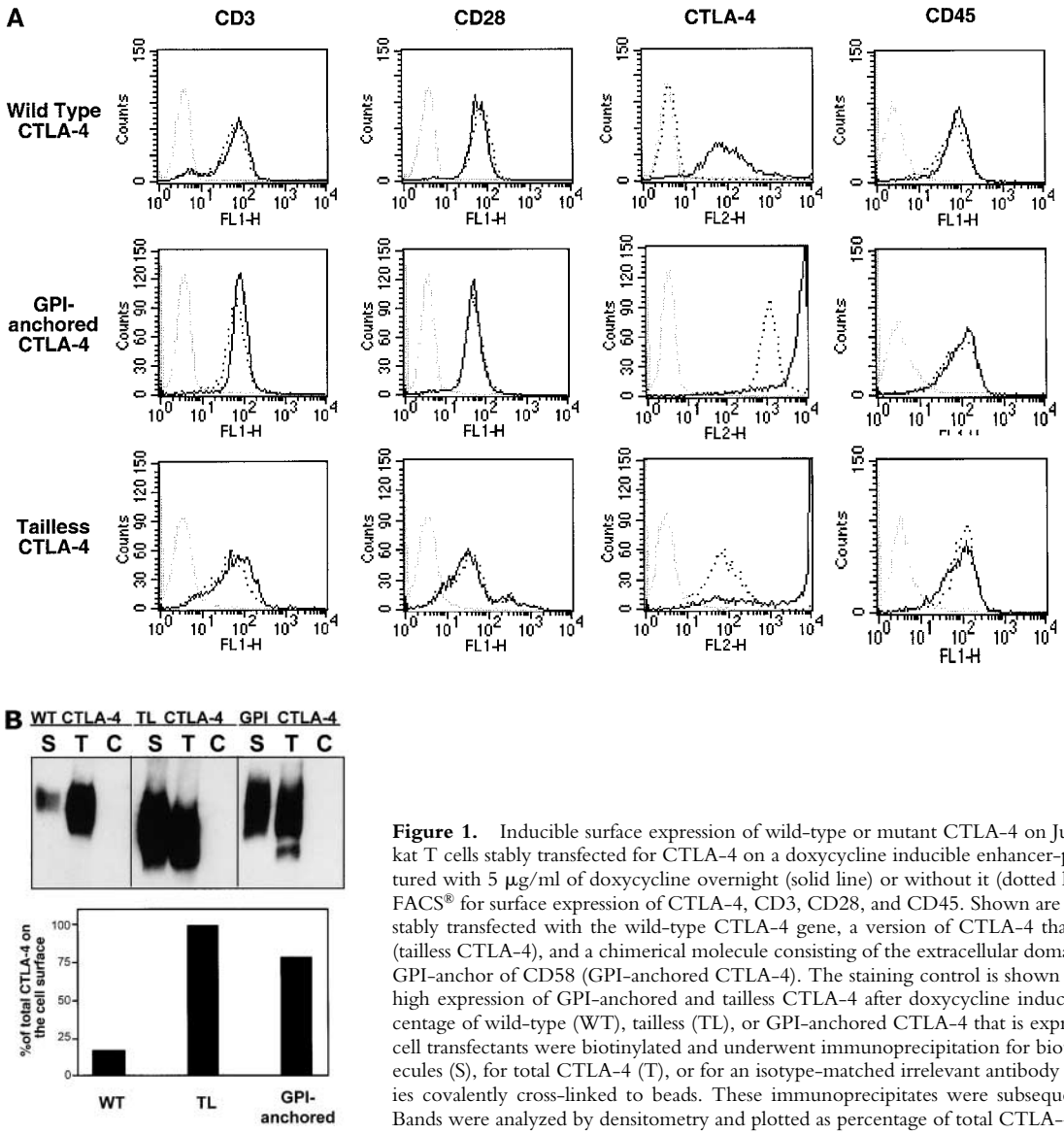

Figure 1. Inducible surface expression of wild-type or mutant CTLA-4 on Jurkat T cell clones. (A) Jurkat T cells stably transfected for CTLA-4 on a doxycycline inducible enhancer-promoter. T cells were cultured with 5 μg/ml of doxycycline overnight (solid line) or without it (dotted line), and were analyzed by FACS® for surface expression of CTLA-4, CD3, CD28, and CD45. Shown are representative T cell clones stably transfected with the wild-type CTLA-4 gene, a version of CTLA-4 that lacks the cytoplasmic tail (tailless CTLA-4), and a chimerical molecule consisting of the extracellular domain of CTLA-4 fused to the GPI-anchor of CD58 (GPI-anchored CTLA-4). The staining control is shown in gray. Note that the very high expression of GPI-anchored and tailless CTLA-4 after doxycycline induction is above 10^4. (B) Percentage of wild-type (WT), tailless (TL), or GPI-anchored CTLA-4 that is expressed on the cell surface. T cell transfectants were biotinylated and underwent immunoprecipitation for biotinylated, i.e., surface, molecules (S), for total CTLA-4 (T), or for an isotype-matched irrelevant antibody control (C), using antibodies covalently cross-linked to beads. These immunoprecipitates were subsequently blotted for CTLA-4. Bands were analyzed by densitometry and plotted as percentage of total CTLA-4 that was biotinylated.

reactivity. The higher levels of the tailless and GPI-anchored mutants are due to inability of these forms to be internalized once they reach the cell surface because of the lack of tyrosine-centered, activating protein 2 (AP-2)–binding sites (35, 36).

Using these CTLA-4 transfectants, we then examined the distribution of surface CTLA-4 in relation to the IS by confocal microscopy (Fig. 2). T cell transfectants were stimulated with the superantigen SEE and an APC expressing high levels of B7 and MHC class II molecules. In the absence of SEE stimulation, both CD3 and CTLA-4 were homogeneously distributed on the surface of the T cells (Fig. 2 A). As the T cells were not permeabilized, no intracellular CTLA-4 was detectable. Upon SEE stimulation, CD3 migrated to the interface between the T cell and APC (Fig. 2 A). LFA-1 and PKCθ also migrated to this area (data not shown), indicating that this interface is a putative IS. More importantly, after doxycycline induction, wild-type CTLA-4 migrated to this interface between T cell and APC and colocalized with CD3 upon stimulation with SEE and APC, conditions that correlate with inhibition of IL-2 production (see below). In addition, CD43 was excluded of the CTLA-4 cluster at the center of the T cell–APC interface (data not shown), supporting the idea that the CTLA-4 cluster is in the immunological synapse. Similar to the wild-type CTLA-4, GPI-anchored CTLA-4 was evenly distributed on the membrane in resting cells and migrated to the IS upon SEE stimulation, where it colocalized with CD3. Tailless CTLA-4 migrated to the IS although the frequency of colocalization with CD3 was lower than that seen with wild-type CTLA-4 as well as with GPI-anchored CTLA-4 as shown by quantification of CD3-CTLA-4 cocapping under conditions of doxycycline induction and coligation induced by SEE and APC (Fig. 2 A). For the GPI-anchored CTLA-4 transfectants and the tailless CTLA-4 transfectants, we show these experiments

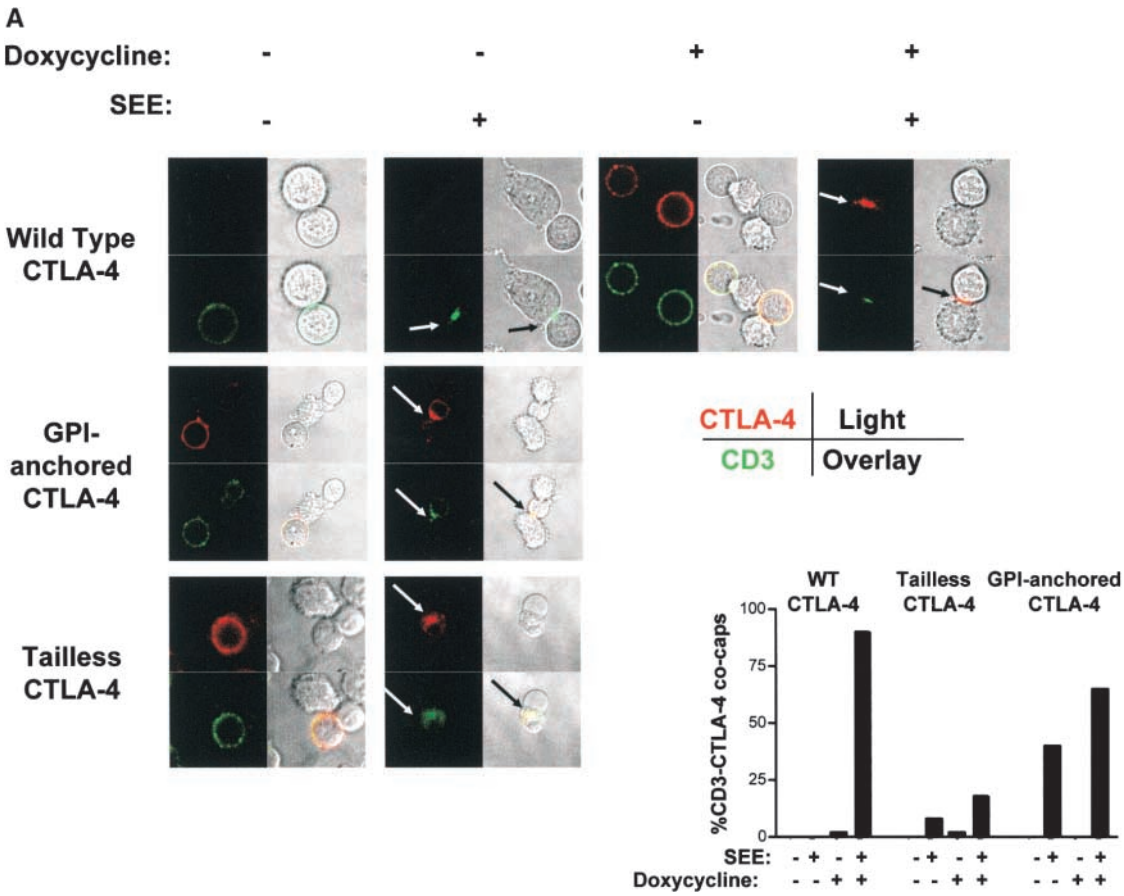

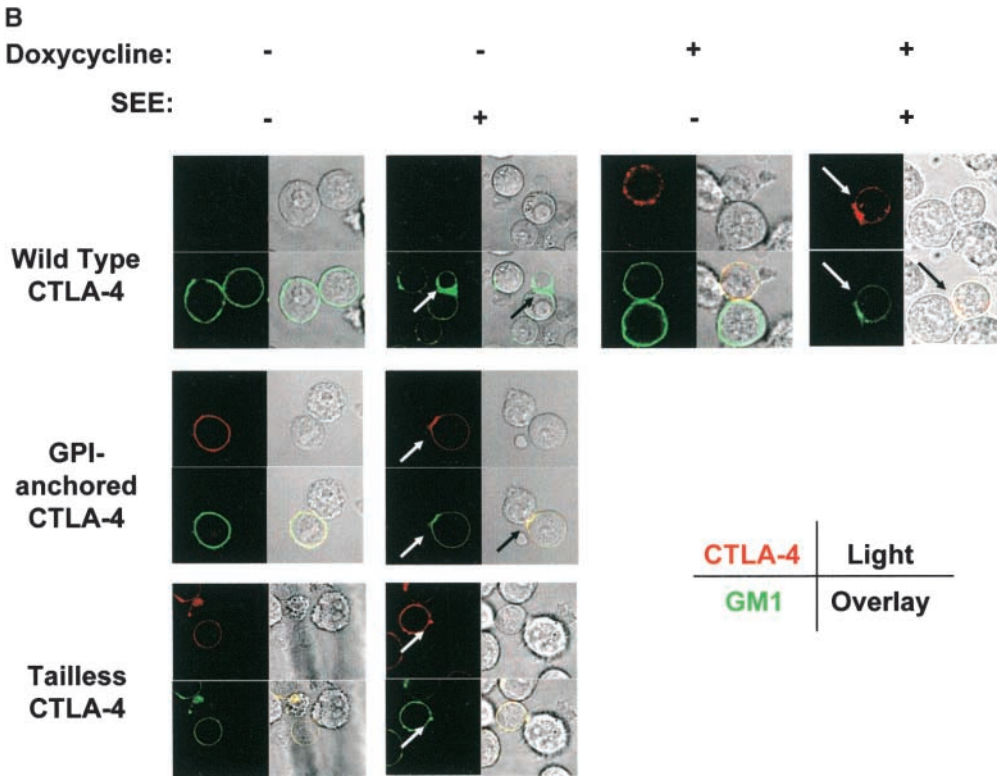

Figure 2. CTLA-4 colocalizes in the IS with CD3 and GM1. Wild-type CTLA-4 transfected Jurkat T cells were induced with doxycycline or noninduced and incubated on poly-L-lysine coated confocal dishes with APC plus 100 ng/ml SEE where indicated. Similarly, tailless and GPI-anchored CTLA-4 in the absence of doxycycline (as these cells express significant amounts of CTLA-4 without it) were used. The samples were put on ice to prevent receptor internalization and immunostained for (A) CD3 (green) and CTLA-4 (red) or (B) GM1 (green) and CTLA-4 (red). The samples were then analyzed by confocal microscopy. Co-capping of CD3 and CTLA-4 was scored when both colocalized at the interface between T cell and APC and the cluster stained <50% of the cell surface. At least 100 doublets per group were counted and scored and results are shown at the bottom right of Fig. 2 A. APCs were identified based on their morphology and lack of staining for CTLA-4 and CD3. Light field pictures were taken simultaneously and merged with the color fields. Yellow indicates overlay of red and green signals.

in the absence of doxycycline induction, as under these conditions, the level of CTLA-4 expression on the surface is more comparable.

Next, we examined the localization of surface CTLA-4 in relation to lipid rafts. The ganglioside GM1, enriched in lipid rafts, was used as a marker for these microdomains. It had been previously shown that GM1 migrates to the point of TCR engagement (7). Consistent with these reports, we found that GM1 became enriched in the IS upon stimulation with SEE. We found that both wild-type and GPI-anchored CTLA-4 colocalized with GM1 (Fig. 2 B). Again, in the tailless CTLA-4–transfected T cells, GM1 did not migrate to the synapse as frequently (Fig. 2 B). These results indicate that under conditions of TCR-CTLA-4 coligation, CTLA-4 relocates to the IS.

Most CTLA-4 Within Lipid Rafts Is on the T Cell Surface. The colocalization of CTLA-4 and GM1 observed by confocal microscopy is only suggestive that CTLA-4 might be found in lipid rafts. To confirm this prediction, we looked for the presence of CTLA-4 within lipid rafts using an established subcellular fractionation protocol (8). Lipid rafts are defined as detergent insoluble, low density compartments which are enriched for GM1, src-kinases such as lck, and LAT, and exclude CD45 and the cytosolic kinases ERK-1/-2 both found in high density soluble fractions (8, 9) (P. Darlington and J. Madrenas, personal observation). When lipid rafts from resting, wild-type CTLA-4–expressing T cell transfectants were analyzed by gel electrophoresis under reducing conditions, ~5–10% of the total amount of CTLA-4 was in lipid rafts while most CTLA-4 was within the soluble fraction (Fig. 3 A). In contrast, only 2% of the total amount of tailless CTLA-4 was found in rafts. In terms of total levels, there was 3.6 times more wild-type CTLA-4 than tailless CTLA-4 in lipid rafts as determined by densitometry (Fig. 3 B). The discrepancy between the amount of wild-type versus tailless CTLA-4 in the rafts is striking considering that the surface expression of tailless CTLA-4 is more than 100 times higher than that of wild-type CTLA-4 (Fig. 1). The quality of the lipid raft fractionation procedure was documented by the selective compartmentalization of GM1 within lipid rafts and of ERK-1/-2 and CD45 within the soluble fractions (Fig. 3 C). Thus, confocal microscopy and subcellular fractionation demonstrate that CTLA-4 can be seen within lipid rafts in a cytoplasmic tail-dependent manner. The finding that CD45, a transmembrane molecule highly expressed on T cells (37), was found mostly in the soluble fraction indicates that high levels of expression of a molecule does not determine its nonspecific localization within lipid rafts. As expected based on the raft localization of other GPI-anchored molecules, the GPI-anchored CTLA-4 was predominantly in the lipid rafts. The magnitude of raft-association of GPI-anchored CTLA-4 rules out the possibility that exclusion from rafts of tailless CTLA-4 is due to a limiting capacity of these microdomains to accommodate more molecules.

As the functional pool of CTLA-4 is primarily that on the cell surface, we determined whether or not the CTLA-4

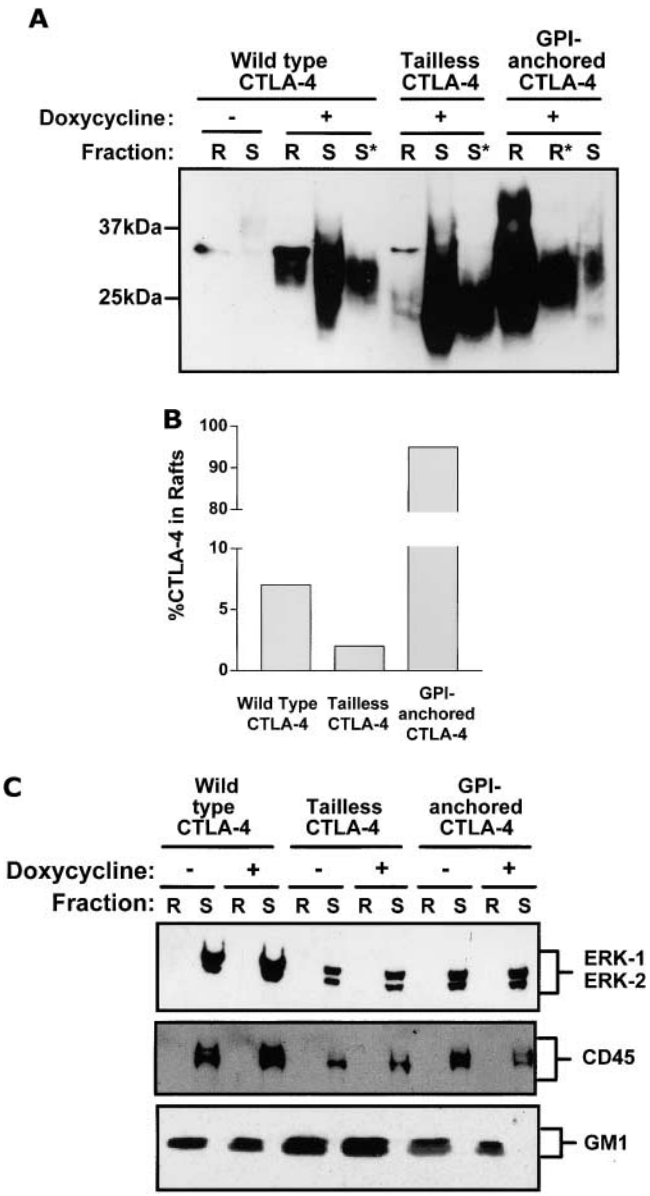

Figure 3. Wild-type CTLA-4 is within lipid rafts in a tail-dependent manner. Lipid raft (R) and detergent-soluble (S) fractions were isolated from resting Jurkat T cells transfected with wild-type CTLA-4, tailless CTLA-4, or GPI-anchored CTLA-4 molecules induced with doxycycline or left noninduced. (A) Selected fractions were run on SDS PAGE and Western blotted for CTLA-4. Where indicated by an asterisk (*) the samples were diluted 10-fold with 1× sample buffer before loading in order to assess nonsaturated signals for CTLA-4 in these samples. CTLA-4 is detected as a broad band attributed to differential glycosylation and intermediate GPI-anchored molecules. (B) Band intensities from the film in panel A were quantified by densitometry and used to calculate the percentage of total CTLA-4 within lipid rafts (see Materials and Methods). (C) The fractions used in the experiment (A) were immunoblotted for ERK-1/-2, CD45, and GM1 to control for quality of the separation. ERK-1/-2 and CD45 were found in the soluble fraction while GM1 partitioned within lipid rafts.

found within lipid rafts was from the surface. To track surface-CTLA-4, uninduced and doxycycline-induced Jurkat T cell transfectants were biotinylated. Next, biotinylated (surface) molecules from lipid raft and soluble frac-

tions were immunoprecipitated, and blotted for CTLA-4. In these experiments, we found that most wild-type CTLA-4 on the cell surface was located in lipid raft fractions while the majority of biotinylated, GPI-anchored CTLA-4 was within lipid rafts and all the biotinylated tailless CTLA-4 was found in the soluble fraction (Fig. 4 A). This approach may have underestimated the amount of surface CTLA-4 in the soluble fraction due to saturation of the anti-biotin immunoprecipitating antibody with other biotinylated molecules. To assess this possibility, we performed avidin blotting of CTLA-4 immunoprecipitates of subcellular fractions. This blotting strategy showed that there was biotinylated CTLA-4 within the soluble fraction. However, when correcting the avidin signals for the CTLA-4 signal in each fraction, we found that the ratio of biotinylated (i.e., surface) CTLA-4 over total CTLA-4 in lipid rafts was higher (82%) than in the soluble fraction (24%; Fig. 4 B). Therefore, we can conclude that most CTLA-4 partitioning within lipid rafts is located on the cell surface.

To assess the biological relevance of the raft-associated pool of wild-type CTLA-4, we determined the presence of CTLA-4 dimers in the raft and soluble fractions, as these are the potentially functional forms of this molecule. A 50-kD band with CTLA-4 immunoreactivity was detectable when CTLA-4 immunoprecipitates from rafts were immunoblotted in nonreducing conditions (Fig. 5). This finding suggests that the CTLA-4 molecules found in lipid rafts are potentially functional.

The Amount of CTLA-4 Within Cell Surface Lipid Rafts Increases Under Conditions of CTLA-4–mediated Inhibition of T Cell Activation. The current model of IS formation proposes that lipid rafts cluster in the IS after T cell stimulation, and provide the permissive environment to sustain early TCR-dependent signaling (6). Thus, we examined the effect of TCR-mediated T cell activation on the distribution of CTLA-4 in lipid rafts. After stimulation of wild-type CTLA-4–expressing T cells with SEE plus APC, we detected an increase in the total levels of CTLA-4 within the lipid rafts (Fig. 6 A). When the cells were biotinylated after stimulation we found that the biotinylated CTLA-4 increased dramatically in lipid raft fractions (Fig. 6 B). No significant change in the levels of CTLA-4 was observed in the soluble fraction upon SEE plus APC stimulation (Fig. 6, A and B). Under these conditions, there was significant inhibition of IL-2 production in response to SEE (Fig. 6 C). This inhibition was significantly released when engagement of CTLA-4 was blocked with soluble single chain antibody against CTLA-4 ($P < 0.05$ by analysis of variance [ANOVA]; Fig. 6 D). Consistent with what we have re-

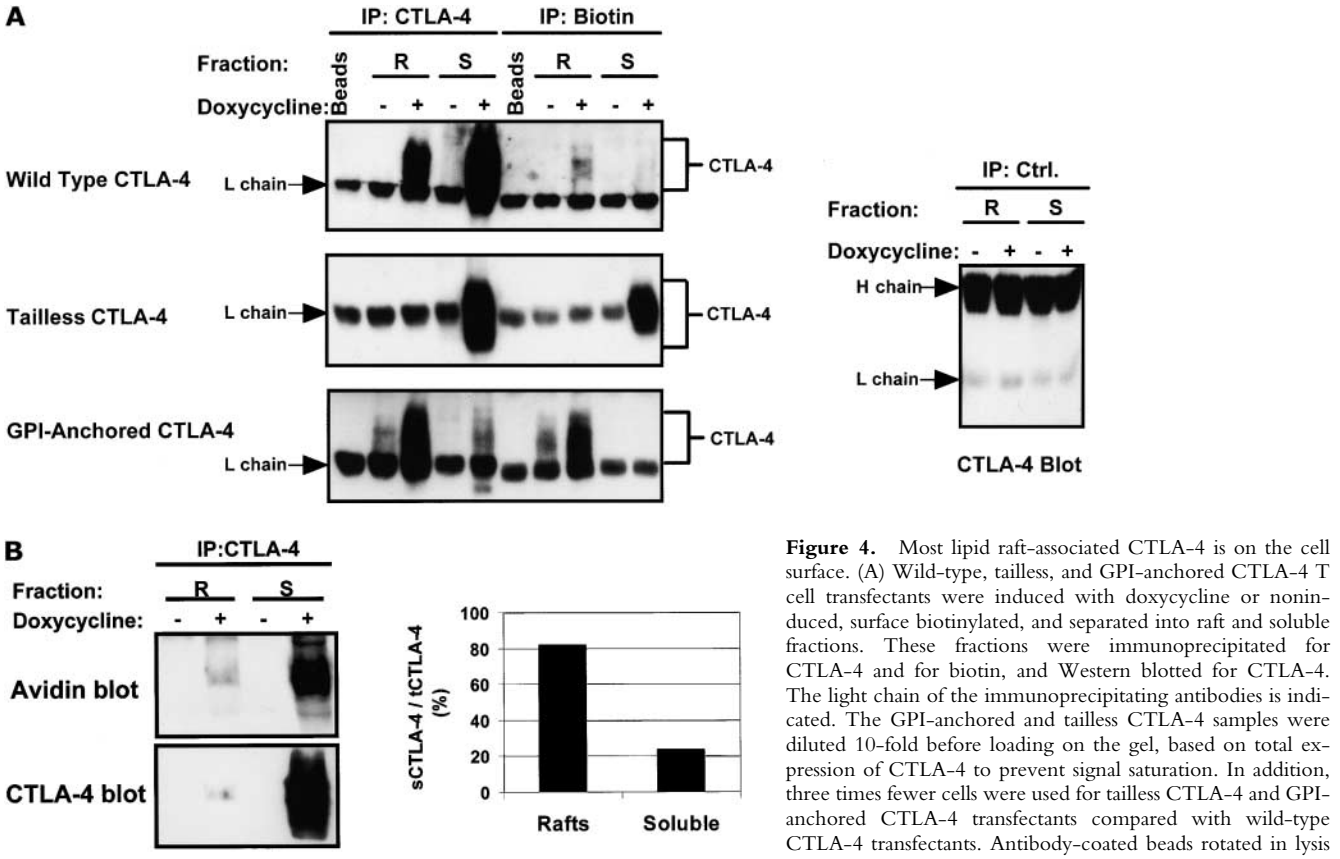

Figure 4. Most lipid raft-associated CTLA-4 is on the cell surface. (A) Wild-type, tailless, and GPI-anchored CTLA-4 T cell transfectants were induced with doxycycline or noninduced, surface biotinylated, and separated into raft and soluble fractions. These fractions were immunoprecipitated for CTLA-4 and for biotin, and Western blotted for CTLA-4. The light chain of the immunoprecipitating antibodies is indicated. The GPI-anchored and tailless CTLA-4 samples were diluted 10-fold before loading on the gel, based on total expression of CTLA-4 to prevent signal saturation. In addition, three times fewer cells were used for tailless CTLA-4 and GPI-anchored CTLA-4 transfectants compared with wild-type CTLA-4 transfectants. Antibody-coated beads rotated in lysis buffer are shown as negative control. Representative isotype-matched control antibody immunoprecipitations (Ctrl.) are shown. (B) CTLA-4 immunoprecipitates of lipid raft and soluble fractions from noninduced and induced, biotinylated wild-type CTLA-4 transfected T cells were sequentially immunoblotted with avidin and with anti–CTLA-4 antibody. Signals were quantified and the ratio of biotinylated CTLA-4 (sCTLA-4) over total CTLA-4 (tCTLA-4) for each fraction plotted in percentage.

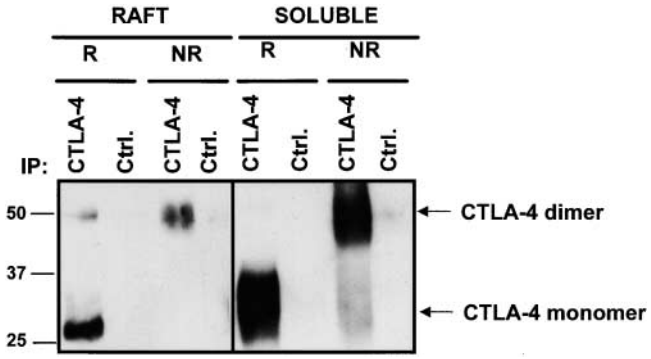

Figure 5. CTLA-4 in lipid rafts is homodimeric. Lipid rafts and soluble fractions from doxycycline induced and noninduced wild-type CTLA-4 T cell transfectants were immunoprecipitated for CTLA-4 or an isotype-matched irrelevant control (Ctrl.). Immunoprecipitates were analyzed by SDS PAGE in nonreducing conditions (NR) and reducing (R) conditions, and Western blotted for CTLA-4.

ported previously (20, 24), expression of surface CTLA-4 upon SEE stimulation for 30 min was slightly increased (Fig. 6 E) but did not affect the total levels of LAT, GM1, or lck within lipid rafts (data not shown). These results demonstrate that surface CTLA-4 is preferentially located within lipid rafts under conditions of inhibition of T cell activation.

Location of CTLA-4 Within Lipid Rafts Is Required But Not Sufficient for CTLA-4–mediated Negative Signaling. Next, we determined whether or not the ability of CTLA-4 to negatively signal correlated with its membrane compartmentalization. One could argue that localization of CTLA-4 in lipid rafts may be sufficient to interfere with TCR-mediated signaling upon coligation by causing physical disruption of the IS. To test this hypothesis we stimulated the different T cell transfectants with immobilized monoclonal antibodies against CD3 or against CD3 and CTLA-4 on beads in the presence of excess costimulation provided by soluble anti-CD28 mAbs. Our group has previously reported that coligation of TCR and wild-type CTLA-4 results in inhibition of ERK1/ERK2 phosphorylation and of IL-2 production, while tailless CTLA-4 does not cause such inhibition by negative signaling (20, 24). As expected, we confirmed that coligation of CD3 and wild-type-CTLA-4 caused significant inhibition of IL-2 production (Fig. 7 A). Blockade of CTLA-4 coligation prevented the inhibition of IL-2 production under these conditions, suggesting that CTLA-4 is responsible for this effect (Fig. 7 B). However, the GPI-anchored-CTLA-4, like we have previously reported for tailless CTLA-4 (20), failed to inhibit T cell activation by negative signaling upon coligation with CD3 and CD28 (Fig. 7 A), despite its almost exclusive localization within lipid rafts. Taken together these results demonstrate that while raft localization may be necessary for inhibition to occur, it is not sufficient to mediate negative signaling.

Discussion

In this study, we show for the first time the membrane compartmentalization of CTLA-4 in T lymphocytes under conditions of CTLA-4–mediated inhibition of T cell activation. Our data demonstrate that a significant fraction of surface CTLA-4 compartmentalizes in the lipid rafts and accumulates at the IS with CD3 and GM1. Such compartmentalization is determined by the cytoplasmic tail of CTLA-4. From a functional point of view, coligation of

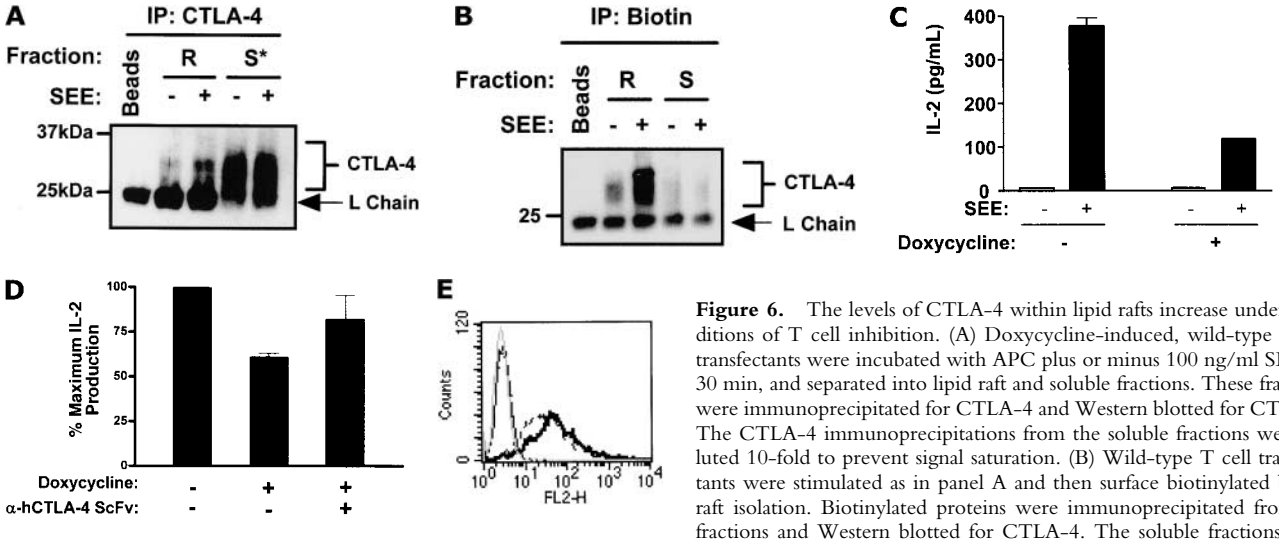

Figure 6. The levels of CTLA-4 within lipid rafts increase under conditions of T cell inhibition. (A) Doxycycline-induced, wild-type T cell transfectants were incubated with APC plus or minus 100 ng/ml SEE for 30 min, and separated into lipid raft and soluble fractions. These fractions were immunoprecipitated for CTLA-4 and Western blotted for CTLA-4. The CTLA-4 immunoprecipitations from the soluble fractions were diluted 10-fold to prevent signal saturation. (B) Wild-type T cell transfectants were stimulated as in panel A and then surface biotinylated before raft isolation. Biotinylated proteins were immunoprecipitated from the fractions and Western blotted for CTLA-4. The soluble fractions were not diluted before loading. (C) Wild-type T cell transfectants were stimulated with SEE and APC for 48 h in the absence (−) or presence (+) of doxycycline to induce CTLA-4 expression. The amount of IL-2 in the supernatant was determined by ELISA. (D) Doxycycline induced Jurkat T cells were preincubated with or without anti–human CTLA-4 ScFv F′ab blocking single chain fragment for 30 min. Then, APCs and SEE were added to the cells and IL-2 production was measured after 48 h. Results were statistically significant as analyzed by one-way ANOVA ($P < 0.05$). (E) Non-induced and doxycycline-induced wild-type–transfected Jurkat T cells were stimulated with APC and SEE for 30 min and CTLA-4 expression on the cell surface was analyzed by flow cytometry. (Non-induced, nonstimulated, control antibody: light dotted line; noninduced, nonstimulated, CTLA-4 stained: thin line; doxycycline-induced, nonstimulated cells: dashed line; doxycycline-induced, stimulated cells: thick line.

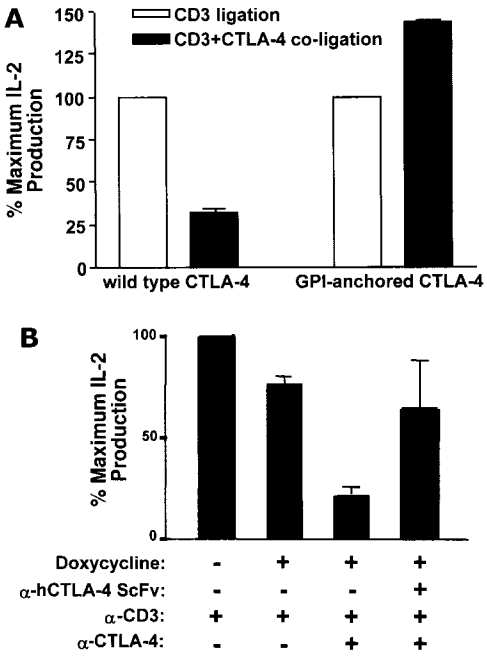

Figure 7. Wild-type CTLA-4, but not GPI-anchored CTLA-4, inhibits IL-2 production upon coligation with the TCR. (A) Wild-type CTLA-4 and GPI-anchored CTLA-4 were incubated with or without 100 ng/ml doxycycline, and incubated with anti-CD3 or anti-CD3 plus anti–CTLA-4 coated beads and soluble anti-CD28 for 48 h. IL-2 in the supernatant was determined by ELISA. The percentage change in IL-2 production in response to anti-CD3 plus anti-CTLA-4 is shown as a bar graph. The response to anti-CD3 beads was taken as 100% for each transfectant. (B) Doxycycline-induced Jurkat T cells were preincubated with or without blocking anti-CTLA-4 ScFv F′ab. After 30 min, beads coated with the indicated antibodies were added to the cells in the presence of soluble anti-CD28 antibodies. IL-2 production was measured after 48 h. Result were statistically significant as analyzed by one-way ANOVA ($P < 0.05$).

CTLA-4 with the TCR is associated with an increase in the levels of CTLA-4 within lipid rafts. However, ligation of CTLA-4 within lipid rafts is not sufficient to inactivate T cells by CTLA-4–mediated signaling.

Compartmentalization of CTLA-4 on the T cell surface has been difficult to examine given the low level of CTLA-4 expression in primary, activated T cells. This forced us to generate a panel of Jurkat T cells expressing high levels of wild-type CTLA-4 upon doxycycline induction. In this way, we achieved sufficient surface CTLA-4 for biochemical, functional, and microscopy studies. More importantly, as Jurkat T cells do not express endogenous CTLA-4, these cells are ideal to assess the structural requirements for CTLA-4 compartmentalization using mutant molecules such as the ones reported here (tailless CTLA-4, GPI-anchored CTLA-4). An additional advantage of the system used in these studies is that we were able to examine the surface compartmentalization under conditions of APC-driven T cell stimulation, making the stimulation conditions more physiologically relevant than previously used monoclonal antibody stimulation.

The recently reported crystal structures of CTLA-4 have led to the proposal that, upon ligation by B7 homodimers, CTLA-4 could form a lattice-like structure whose intermembrane dimension (100–140 Å) might be accommodated within the IS (29–32). Our finding of CTLA-4 in the IS is consistent with this model. Furthermore, our data indicate that this lattice does not grossly disrupt the morphology of the IS. This is particularly significant for the TCR complex, as one could claim that the negative function of CTLA-4 may be through interference with TCR oligomerization at the IS. Our findings stress the concept that CTLA-4 and CD3 have to be physically coligated for negative signaling to occur, consistent with the data indicating that such coligation is only functional when in cis, i.e., both ligands on the same surface (20, 24, 33). Future studies will be required to determine the effect that CTLA-4 may have on the fine stoichiometry and organization of the IS.

We have also analyzed the compartmentalization of CTLA-4 with respect to lipid rafts. The majority of CTLA-4 was outside of lipid rafts. However, a significant fraction of total CTLA-4 was within lipid rafts. The cytoplasmic tail of CTLA-4 was required for its efficient localization within lipid rafts, a novel finding indicating that the cytoplasmic region and not the transmembrane region alone (which is present in the tailless CTLA-4) is critical for raft association. The exact residues within the tail responsible for the lipid raft localization are unknown. As expected from previous reports of GPI-anchored molecules being enriched in lipid rafts (38, 39), a GPI-anchored version of CTLA-4 was found mostly in these microdomains.

The physiological relevance of lipid raft-associated CTLA-4 is currently unknown. As CTLA-4 in lipid rafts can be found as homodimers and clusters to the IS, it is plausible to assume that the pool within lipid rafts is functional. More importantly, the observation that the content of CTLA-4 within lipid rafts increased under conditions of CTLA-4–mediated inhibition further supports this claim. Such an increase may be explained by retention of CTLA-4 on the cell surface upon TCR ligation or alternatively, by a net increase of CTLA-4 migration into lipid rafts.

The compartmentalization of CTLA-4 within lipid rafts has implications for the search of CTLA-4 targets and/or regulators since one would expect that such molecules are located in these microdomains. Our data are compatible with the model proposing that TCR-ζ is the target of CTLA-4 as the phosphorylated form of this chain has been found in lipid rafts (26). However, it should be noted that in the T cell system described in this report, we have not been able to detect CTLA-4 associated with TCR-ζ or SHP-2 (unpublished data). We and others favor an effect of CTLA-4 on ERK activation and JNK signaling (23, 24, 28), which is also consistent with the lipid raft compartmentalization of CTLA-4, as lipid rafts are enriched in LAT and ras (8, 9). Similar considerations apply to regulators of CTLA-4 function such as the regulatory subunit of the serine/threonine phosphatase PP2A (39a). Therefore, the presence of the regulatory machinery of CTLA-4 func-

tion and of the potential targets of this molecule within lipid rafts argues that the lipid raft-associated fraction of CTLA-4 is biologically important.

As most of the lipid raft-associated CTLA-4 is on the cell surface, and this pool increases after coligation with the TCR, we propose that raft localization is necessary for CTLA-4–mediated negative signaling. In support of this claim is the data that tailless CTLA-4 that is mostly outside lipid rafts failed to inhibit T cell activation by negative signaling. However, raft localization of CTLA-4 is not sufficient for CTLA-4–mediated negative signaling, as the GPI-anchored CTLA-4 that is almost exclusively in lipid rafts and migrates to the IS did not inhibit T cell activation. We cannot exclude fine molecular differences in the lattice formed by the GPI-anchored CTLA-4 compared with that formed by the wild-type CTLA-4. However, the suggestion of lattice formation was made from crystals in which only the extracellular domain of CTLA-4 was used, and thus it is plausible to assume that lattice formation may be primarily determined by the extracellular portion of CTLA-4.

The results of this study can be incorporated into a broader model of CTLA-4 trafficking. The majority of CTLA-4 in a resting, previously activated T cell would be primarily in intracellular, detergent soluble compartments where it is constantly being shuttled to the surface, where it compartmentalizes in lipid rafts. This pool is reinternalized via an AP-2–dependent process (21, 36). The localization within lipid rafts may facilitate that process, as it is well established that lipid rafts are involved in internalization (40). Upon TCR ligation, CTLA-4 is tyrosine phosphorylated in a lck and ZAP-70–dependent manner (24). This phosphorylation event prevents AP-2–dependent internalization, and leads to retention of CTLA-4 on the cell surface. In addition, polarization of the intracellular stores of CTLA-4 toward the APC would facilitate its release into the IS (41). The raft-associated CTLA-4 would then cluster in the IS, where it could potentially mediate the formation of extended lattice networks of B7 and CTLA-4 (29). Further studies on the specific contribution of the cytoplasmic tail and lipid raft compartmentalization to CTLA-4 relocation into the IS should help us to identify the fine molecular arrangement within this highly organized interface.

We thank Luan A. Chau and Elizabeth M. Tomas for technical comments and all the members of the Madrenas Laboratory for helpful criticisms.

This work was supported by grants from the Canadian Institutes of Health Research, the Kidney Foundation of Canada, and Wyeth-Genetics Institute Inc. E. Siu holds a Natural Sciences and Engineering Research Council of Canada post-graduate scholarship. J. Madrenas holds a Canada Research Chair in Transplantation and Immunobiology.

Submitted: 8 November 2001
Revised: 27 March 2002
Accepted: 8 April 2002

References

1. Bromley, S.K., W.R. Burack, K.G. Johnson, K. Somersalo, T.N. Sims, C. Sumen, M.M. Davis, A.S. Shaw, P.M. Allen, and M.L. Dustin. 2001. The immunological synapse. *Annu. Rev. Immunol.* 19:375–396.
2. Monks, C.R., H. Kupfer, I. Tamir, A. Barlow, and A. Kupfer. 1997. Selective modulation of protein kinase C-theta during T-cell activation. *Nature.* 385:83–86.
3. Monks, C.R., B.A. Freiberg, H. Kupfer, N. Sciaky, and A. Kupfer. 1998. Three-dimensional segregation of supramolecular activation clusters in T cells. *Nature.* 395:82–86.
4. Delon, J., K. Kaibuchi, and R.N. Germain. 2001. Exclusion of CD43 from the immunological synapse is mediated by phosphorylation-regulated relocation of the cytoskeletal adaptor moesin. *Immunity.* 15:691–701.
5. Shaw, A.S. 2001. FERMing up the synapse. *Immunity.* 15: 683–686.
6. Dustin, M.L., and J.A. Cooper. 2000. The immunological synapse and the actin cytoskeleton: molecular hardware for T cell signaling. *Nat. Immunol.* 1:23–29.
7. Viola, A., S. Schroeder, Y. Sakakibara, and A. Lanzavecchia. 1999. T lymphocyte costimulation mediated by reorganization of membrane microdomains. *Science.* 283:680–682.
8. Xavier, R., T. Brennan, Q. Li, C. McCormack, and B. Seed. 1998. Membrane compartmentation is required for efficient T cell activation. *Immunity.* 8:723–732.
9. Zhang, W., R.P. Trible, and L.E. Samelson. 1998. LAT palmitoylation: its essential role in membrane microdomain targeting and tyrosine phosphorylation during T cell activation. *Immunity.* 9:239–246.
10. Bi, K., Y. Tanaka, N. Coudronniere, K. Sugie, S. Hong, M.J. van Stipdonk, and A. Altman. 2001. Antigen-induced translocation of PKC-theta to membrane rafts is required for T cell activation. *Nat. Immunol.* 2:556–563.
11. Kabouridis, P.S., J. Janzen, A.L. Magee, and S.C. Ley. 2000. Cholesterol depletion disrupts lipid rafts and modulates the activity of multiple signaling pathways in T lymphocytes. *Eur. J. Immunol.* 30:954–963.
12. Brunet, J.F., F. Denizot, M.F. Luciani, M. Roux-Dosseto, M. Suzan, M.G. Mattei, and P. Golstein. 1987. A new member of the immunoglobulin superfamily—CTLA-4. *Nature.* 328:267–270.
13. Walunas, T.L., D.J. Lenschow, C.Y. Bakker, P.S. Linsley, G.J. Freeman, J.M. Green, C.B. Thompson, and J.A. Bluestone. 1994. CTLA-4 can function as a negative regulator of T cell activation. *Immunity.* 1:405–413.
14. Krummel, M.F., and J.P. Allison. 1996. CTLA-4 engagement inhibits IL-2 accumulation and cell cycle progression upon activation of resting T cells. *J. Exp. Med.* 183:2533–2540.
15. Chambers, C.A., T.J. Sullivan, and J.P. Allison. 1997. Lymphoproliferation in CTLA-4-deficient mice is mediated by costimulation-dependent activation of $CD4^+$ T cells. *Immunity.* 7:885–895.
16. Tivol, E.A., F. Borriello, A.N. Schweitzer, W.P. Lynch, J.A. Bluestone, and A.H. Sharpe. 1995. Loss of CTLA-4 leads to massive lymphoproliferation and fatal multiorgan tissue destruction, revealing a critical negative regulatory role of CTLA-4. *Immunity.* 3:541–547.
17. Waterhouse, P., J.M. Penninger, E. Timms, A. Wakeham, A. Shahinian, K.P. Lee, C.B. Thompson, H. Griesser, and T.W. Mak. 1995. Lymphoproliferative disorders with early lethality in mice deficient in Ctla-4. *Science.* 270:985–988.

18. Brunner, M.C., C.A. Chambers, F.K. Chan, J. Hanke, A. Winoto, and J.P. Allison. 1999. CTLA-4-Mediated inhibition of early events of T cell proliferation. *J. Immunol.* 162: 5813–5820.
19. Baroja, M.L., P.J. Darlington, B.M. Carreno, and J. Madrenas. 2000. Inhibition of T cell activation by CTLA-4: truths and red herrings. *Mod. Asp. Immunobiol.* 1:169–173.
20. Carreno, B.M., F. Bennett, T.A. Chau, V. Ling, D. Luxenberg, J. Jussif, M.L. Baroja, and J. Madrenas. 2000. CTLA-4 (CD152) can inhibit T cell activation by two different mechanisms depending on its level of cell surface expression. *J. Immunol.* 165:1352–1356.
21. Thompson, C.B., and J.P. Allison. 1997. The emerging role of CTLA-4 as an immune attenuator. *Immunity.* 7:445–450.
22. van der Merwe, P.A., D.L. Bodian, S. Daenke, P. Linsley, and S.J. Davis. 1997. CD80 (B7-1) binds both CD28 and CTLA-4 with a low affinity and very fast kinetics. *J. Exp. Med.* 185:393–403.
23. Nakaseko, C., S. Miyatake, T. Iida, S. Hara, R. Abe, H. Ohno, Y. Saito, and T. Saito. 1999. Cytotoxic T lymphocyte antigen 4 (CTLA-4) engagement delivers an inhibitory signal through the membrane-proximal region in the absence of the tyrosine motif in the cytoplasmic tail. *J. Exp. Med.* 190:765–774.
24. Baroja, M.L., D. Luxenberg, T. Chau, V. Ling, C.A. Strathdee, B.M. Carreno, and J. Madrenas. 2000. The inhibitory function of CTLA-4 does not require its tyrosine phosphorylation. *J. Immunol.* 164:49–55.
25. Cinek, T., A. Sadra, and J.B. Imboden. 2000. Cutting edge: tyrosine-independent transmission of inhibitory signals by CTLA-4. *J. Immunol.* 164:5–8.
26. Lee, K.M., E. Chuang, M. Griffin, R. Khattri, D.K. Hong, W. Zhang, D. Straus, L.E. Samelson, C.B. Thompson, and J.A. Bluestone. 1998. Molecular basis of T cell inactivation by CTLA-4. *Science.* 282:2263–2266.
27. Schneider, H., K.V. Prasad, S.E. Shoelson, and C.E. Rudd. 1995. CTLA-4 binding to the lipid kinase phosphatidylinositol 3-kinase in T cells. *J. Exp. Med.* 181:351–355.
28. Calvo, C.R., D. Amsen, and A.M. Kruisbeek. 1997. Cytotoxic T lymphocyte antigen 4 (CTLA-4) interferes with extracellular signal-regulated kinase (ERK) and Jun NH2-terminal kinase (JNK) activation, but does not affect phosphorylation of T cell receptor zeta and ZAP70. *J. Exp. Med.* 186:1645–1653.
29. Ostrov, D.A., W. Shi, J.C. Schwartz, S.C. Almo, and S.G. Nathenson. 2000. Structure of murine CTLA-4 and its role in modulating T cell responsiveness. *Science.* 290:816–819.
30. Stamper, C.C., Y. Zhang, J.F. Tobin, D.V. Erbe, S. Ikemizu, S.J. Davis, M.L. Stahl, J. Seehra, W.S. Somers, and L. Mosyak. 2001. Crystal structure of the B7-1/CTLA-4 complex that inhibits human immune responses. *Nature.* 410:608–611.
31. Schwartz, J.C., X. Zhang, A.A. Fedorov, S.G. Nathenson, and S.C. Almo. 2001. Structural basis for co-stimulation by the human CTLA-4/B7-2 complex. *Nature.* 410:604–608.
32. Davis, S.J., S. Ikemizu, A.V. Collins, J.A. Fennelly, K. Harlos, E.Y. Jones, and D.I. Stuart. 2001. Crystallization and functional analysis of a soluble deglycosylated form of the human costimulatory molecule B7-1. *Acta Crystallogr. D Biol. Crystallogr.* 57:605–608.
33. Blair, P.J., J.L. Riley, B.L. Levine, K.P. Lee, N. Craighead, T. Francomano, S.J. Perfetto, G.S. Gray, B.M. Carreno, and C.H. June. 1998. CTLA-4 ligation delivers a unique signal to resting human CD4 T cells that inhibits interleukin-2 secretion but allows Bcl-X(L) induction. *J. Immunol.* 160:12–15.
34. Chau, L.A., J.A. Bluestone, and J. Madrenas. 1998. Dissociation of intracellular signaling pathways in response to partial agonist ligands of the T cell receptor. *J. Exp. Med.* 187:1699–1709.
35. Shiratori, T., S. Miyatake, H. Ohno, C. Nakaseko, K. Isono, J.S. Bonifacino, and T. Saito. 1997. Tyrosine phosphorylation controls internalization of CTLA-4 by regulating its interaction with clathrin-associated adaptor complex AP-2. *Immunity.* 6:583–589.
36. Zhang, Y., and J.P. Allison. 1997. Interaction of CTLA-4 with AP50, a clathrin-coated pit adaptor protein. *Proc. Natl. Acad. Sci. USA.* 94:9273–9278.
37. Trowbridge, I.S., and M.L. Thomas. 1994. CD45: an emerging role as a protein tyrosine phosphatase required for lymphocyte activation and development. *Annu. Rev. Immunol.* 12:85–116.
38. Varma, R., and S. Mayor. 1998. GPI-anchored proteins are organized in submicron domains at the cell surface. *Nature.* 394:798–801.
39. Friedrichson, T., and T.V. Kurzchalia. 1998. Microdomains of GPI-anchored proteins in living cells revealed by crosslinking. *Nature.* 394:802–805.
39a. Baroja, M.L., L. Vijayakrishnan, E. Bettelli, P.J. Darlington, T.A. Chau, V. Ling, M. Collins, B.M. Carreno, J. Madrenas, and V.J. Kuchroo. 2002. Inhibition of CTLA-4 function by the regulatory subunit of serine/threonine phosphatase 2A. *J. Immunol.* In press.
40. Simons, K., and E. Ikonen. 1997. Functional rafts in cell membranes. *Nature.* 387:569–572.
41. Linsley, P.S., J. Bradshaw, J. Greene, R. Peach, K.L. Bennett, and R.S. Mittler. 1996. Intracellular trafficking of CTLA-4 and focal localization towards sites of TCR engagement. *Immunity.* 4:535–543.